

THE OFFICIAL MAGAZINE OF THE OCEANOGRAPHY SOCIETY

Oceanography

CITATION

Faye, S., A. Rochon, and G. St-Onge. 2018. Distribution of modern dinoflagellate cyst assemblages in surface sediments of San Jorge Gulf (Patagonia, Argentina). *Oceanography* 31(4):122–131, <https://doi.org/10.5670/oceanog.2018.416>.

DOI

<https://doi.org/10.5670/oceanog.2018.416>

PERMISSIONS

Oceanography (ISSN 1042-8275) is published by The Oceanography Society, 1 Research Court, Suite 450, Rockville, MD 20850 USA. ©2018 The Oceanography Society, Inc. Permission is granted for individuals to read, download, copy, distribute, print, search, and link to the full texts of *Oceanography* articles. Figures, tables, and short quotes from the magazine may be republished in scientific books and journals, on websites, and in PhD dissertations at no charge, but the materials must be cited appropriately (e.g., authors, *Oceanography*, volume number, issue number, page number[s], figure number[s], and DOI for the article).

Republication, systemic reproduction, or collective redistribution of any material in *Oceanography* is permitted only with the approval of The Oceanography Society. Please contact Jennifer Ramarui at info@tos.org.

Permission is granted to authors to post their final pdfs, provided by *Oceanography*, on their personal or institutional websites, to deposit those files in their institutional archives, and to share the pdfs on open-access research sharing sites such as ResearchGate and Academia.edu.

Distribution of Modern Dinoflagellate Cyst Assemblages in Surface Sediments of San Jorge Gulf (Patagonia, Argentina)

By Simon Faye, André Rochon, and Guillaume St-Onge



ABSTRACT. The presence of upwelling systems and oceanic fronts makes the Southwest Atlantic Ocean a region of high primary productivity. These same conditions are present in San Jorge Gulf (SJG) along the southern Argentinian coast, where dinoflagellates and diatoms dominate primary production. The distribution of these microorganisms, including the cysts produced by some dinoflagellates during their life cycles, is controlled in marine environments by oceanographic parameters that include salinity, surface water temperature, ice cover duration, and productivity. The objective of this study is to document the modern distribution of dinoflagellate cyst assemblages in surface sediments so that the environmental preferences of each taxon can be inferred and used to reconstruct paleoenvironmental conditions. The dinoflagellate cyst (dinocyst) assemblages of 52 surface samples collected in 2014 aboard R/V *Coriolis II* in the SJG were described and compared to surface oceanographic conditions and grain size data. The results indicate dinocyst concentrations vary between 64 cysts g^{-1} and 45,848 cysts g^{-1} dry sediment, with *Spiniferites ramosus* and *Operculodinium centrocarpum* the dominant species, accompanied by *Spiniferites mirabilis*, *Dubridinium* sp., cysts of *Polykrikos kofoidii*, and cysts of *Brigantedinium simplex*, *Brigantedinium auranteum*, and *Brigantedinium* spp. We have defined two spatial domains based on the distribution of dinocysts in and near the SJG: northern/southern-central gulf and offshore domains. We found an increase in dinocyst concentrations along a north-south gradient in the SJG and minimum concentrations at offshore sites. In addition, multivariate analyses reveal the relationships among the relative abundances of dinocysts, fine grain size data ($<63 \mu\text{m}$; silts and clays), and primary productivity, as well as offshore upwelling, which appear to control most of the distribution of dinocysts.

INTRODUCTION

The Southwest Atlantic is an area of high primary productivity, where upwellings and oceanic fronts control the intensity of organic production (Gregg et al., 2005; Rivas et al., 2006). Along the Argentinian coasts, dinoflagellates and diatoms dominate the primary production (e.g., Lutz and Carreto, 1991; Segura et al., 2013; Krock et al., 2015). These microorganisms represent the bottom link in the food web and are essential for marine ecosystems.

Dinoflagellates are unicellular biflagellate organisms that thrive in both freshwater and marine environments. They display a wide range of morphologies, live in a variety of habitats (Evitt, 1985; Taylor et al., 2008), and are found at all latitudes, though they are particularly abundant in coastal waters (Zonneveld et al., 2013). Most dinoflagellates are autotrophic and/or mixotrophic (50%), but some are either heterotrophic, parasitic, or

symbiotic (Stoecker, 1999). Autotrophic dinoflagellates form part of the primary production, while heterotrophic species feed primarily on diatoms, nanoflagellates, bacteria, or other dinoflagellates (Jacobson and Anderson, 1986; Hansen, 1992; Jeong et al., 2010). Most dinoflagellates have a cellulosic theca (~89%) that degrades rapidly following cell death. In addition, about 13% to 16% of the species produce a diploid cell surrounded by a resistant organic membrane (cyst) that allows the organism to survive during dormancy (Head, 1996). The organic membrane is composed of dinosporin and appears carbohydrate-based (Versteegh et al., 2012). Those produced by phototrophs are composed of a cellulose-like glucan, while those of heterotrophs are composed of nitrogen-rich glycan (Bogus et al. 2014). During the dormancy phase, the cyst is preserved in the sediments until the environmental conditions become favorable for excystment. During this stage, the diploid cell extrudes from the cyst and may develop (or not, e.g., *Gymnodiniales*) a theca with characteristics specific to each species.

Dinoflagellate cysts (dinocysts) are used in many studies as paleoceanographic proxies for the reconstruction of environmental parameters such as salinity, surface water temperature, ice cover duration, and productivity (e.g., Durantou et al., 2012; de Vernal et al., 2013). However, most studies are located in the North Atlantic (e.g., de Vernal et al., 2013; Zonneveld et al., 2013). In the South Atlantic, the surface distribution of dinocysts is limited to only a few studies (e.g., Wall et al., 1977; Orozco and Carreto, 1989; Esper and Zonneveld, 2002; Candel et al., 2012, Krock et al., 2015). Only one (Krock et al., 2015) is located in San Jorge Gulf (SJG), but it is based on the analysis of five surface sediment samples and thus does not provide a precise distribution of dinocysts in the gulf. In addition, the relationships between cyst assemblages and sea surface conditions were not assessed.

Here, we present the first detailed study

of modern dinoflagellate cyst assemblages in surface sediments from the SJG. The objectives are to analyze dinoflagellate cyst assemblages from 52 surface sediment samples and to establish the surface distribution of each taxon and the relationships between cyst assemblages and sea surface parameters. These modern assemblages will serve as paleoenvironmental indicators of sea surface conditions (temperature, salinity, and productivity) in the gulf and at the offshore upwelling area from the sedimentary record for the Late Pleistocene and the Holocene.

REGIONAL SETTING

The SJG is a shallow oceanic basin (mean depth 70 m) located in the center of Patagonia in the Southwest Atlantic Ocean between 45°S (Cape Dos Bahías) and 47°S (Cape Tres Puntas). It is about 250 km wide and encompasses a total area of 39,000 km² (Glebocki et al., 2015).

Atmospheric circulation in the Patagonia region is strongly influenced by westerlies (Aravena and Luckman, 2009). This area lies between the semi-permanent subtropical high pressure belt and the subpolar low pressure belt. The small differences in atmospheric pressure between these belts control the intensity and direction of winds that influence, among other phenomena, the oceanic circulation on the southwestern continental shelf of Patagonia (Mayr et al., 2007; Palma et al., 2008).

The general ocean circulation in the Southwest Atlantic is characterized by the Malvinas Current (MC), a branch of the Antarctic Circumpolar Current. It flows northward along the edge of the continental slope from Drake Passage (55°S) to 38°S (Palma et al., 2008; Piola et al., 2009; Matano et al., 2010) and transports cold, salty (>34) nutrient-rich subantarctic waters (Piola et al., 2009). On the continental shelf, water masses have much lower salinity (<34) than MC water masses because of the influence of freshwater discharges by rivers (Deseado, San Julian, Coig, and Gallegos) and low-salinity waters carried through the Strait

of Magellan located south of the SJG (Bianchi et al., 2005; Rivas et al., 2006; Figure 1A). The latter are responsible for the presence on the Patagonian shelf of low-salinity coastal waters (<33.4), which extend into the SJG (Bianchi et al., 2005) and generate an intense seasonal thermohaline front in the gulf (Krock et al., 2015). There are also high-salinity coastal waters (~34) near San Matías due to intense evaporation (Bianchi et al., 2005; Figure 1A). Interactions of these different water masses on the Patagonian shelf are particularly important for understanding the characteristics of water masses within the SJG.

According to Krock et al. (2015), SJG water masses are strongly influenced by the high-salinity coastal water in the north and the low-salinity coastal water in the south. The general circulation in the SJG is seasonally variable, exhibiting two distinct patterns, austral summer and winter modes (Matano and Palma, 2018, in this issue). The summer mode, which reflects annual mean patterns, is characterized by a cyclonic gyre that is bound to the west by coastal currents and to the east by the Patagonia Current (PC, Matano et al., 2018, in this issue). The PC is composed mainly of low-salinity, subantarctic waters from the Strait of Magellan (Brandhorst and Castello, 1971). According to Matano and Palma (2018, in this issue), the summer mode is characterized by maximum intrusion of the PC into the gulf, and the cyclonic gyres weaken significantly during the winter mode. Strong winter mode westerlies generate two anticyclonic subgyres, the larger of which is situated in the southwestern gulf and characterized by a southward-flowing coastal current (Matano and Palma, 2018, in this issue). The surface circulation pattern suggests that winds, heat fluxes, the topographic depression in the central part of the gulf, and the seasonal development of tidal fronts control hydrodynamics in the area (Krock et al., 2015; Matano and Palma, 2018, in this issue).

In the interior of the gulf, the waters are highly stratified (Krock et al., 2015),

and warming during austral spring and summer induces thermal fronts that delimit stratified waters (Rivas et al., 2006). This phenomenon is associated with strong tidal currents, which can inhibit the seasonal development of the thermocline, and which generate tidal fronts at the 200 m isobath (Figure 1A; Rivas et al. 2006; Carbajal et al., 2018, in this issue) that are characterized by areas of high primary production (Sabatini

and Martos, 2002). Based on the numerical simulations of Tonini et al. (2006), there is a downwelling system along the northern coastal region and wind-driven upwelling within the south-southwest gulf. We also note the presence along the 200 m isobath of offshore upwelling zones (Matano et al., 2010), whose mechanisms are poorly understood. Some authors have hypothesized that internal friction created by the lateral diffusion of the MC

on the continental shelf could cause this upwelling, rather than external forcings such as winds and tides (Matano et al., 2010). Thus, the cold, nutrient-rich subantarctic waters transported by the MC would be shifted toward the coast from below and then raised to the surface by vertical mixing and returned northward by Ekman transport generated by westerlies (Matano and al., 2010).

Surface sediments in most of the SJG

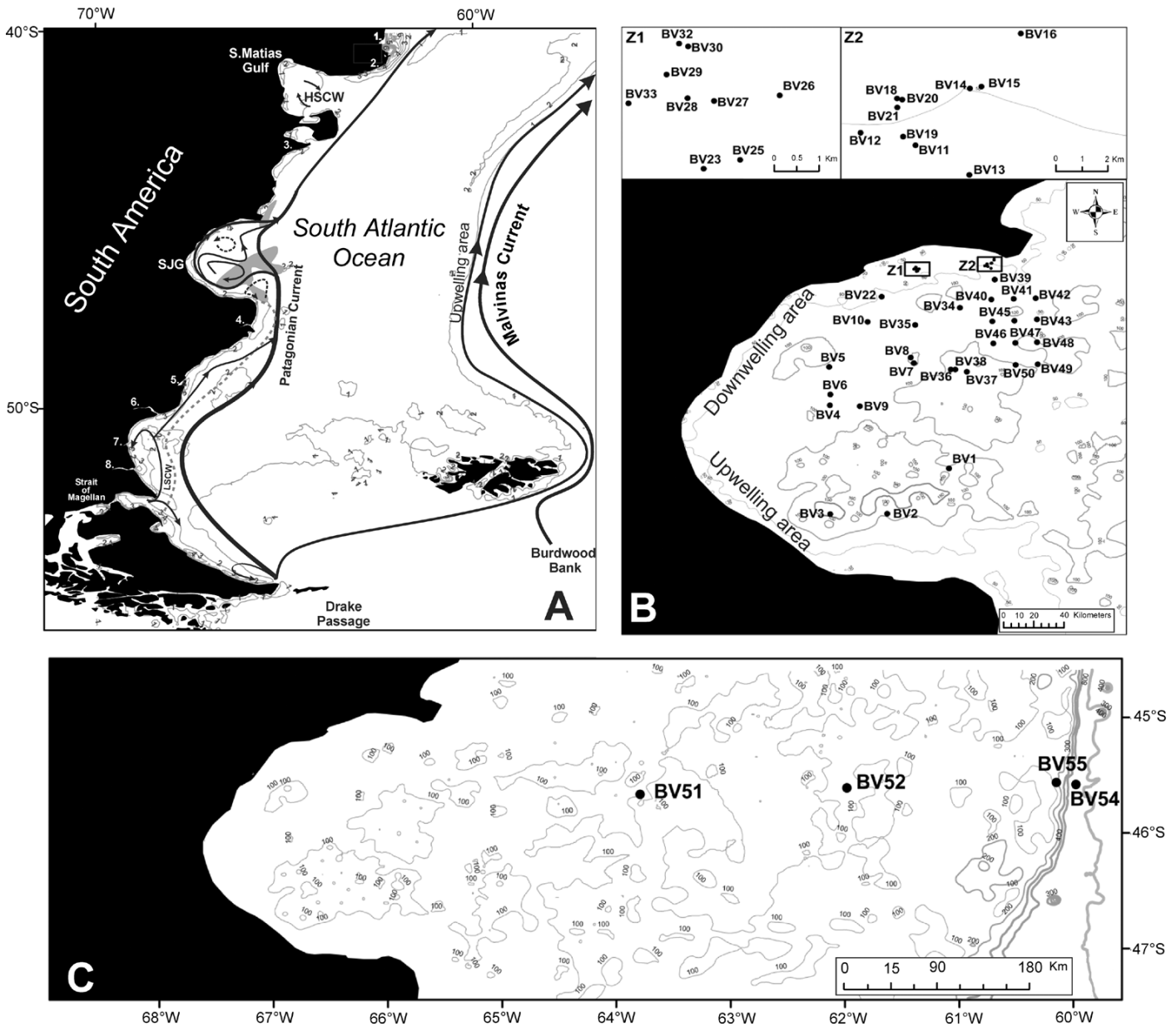


FIGURE 1. (A) Schematic representation of southwestern Atlantic circulation and summer circulation pattern in San Jorge Gulf (SJG; adapted from Matano et al., 2010, and Matano and Palma, 2018, in this issue), showing the Malvinas Current, the Patagonia Current, Low Salinity Coastal Water (LSCW), the Magellan discharge (dashed line), and the High Salinity Coastal Water (HSCW), with a focus on tidal coastal fronts (gray zones) in the SJG. The isolines represent the annual climatological chlorophyll *a* concentrations (mg m^{-3} , Rivas et al., 2006). The Patagonian rivers are indicated: 1. Colorado. 2. Negro. 3. Chubut. 4. Deseado. 5. San Juliàn. 6. Chico. 7. Coig. 8. Gallegos. (B and C) Maps of the SJG illustrating the locations of surface samples analyzed in this study. Isobaths are from the General Bathymetric Chart of the Oceans (GEBCO).

are dominated by silt and clay and are associated with a low energy depositional environment, although coarse sand and energetic erosive environments prevail in the northern gulf (Fernández et al., 2003; Desiage et al., 2018, in this issue).

MATERIAL AND METHODS

Sampling

Collection of 52 surface samples was carried out from R/V *Coriolis II* from February 17 to March 4, 2014, during the MARGES (marine geology, sedimentology, stratigraphy, basin architecture and paleoceanography of San Jorge Gulf) oceanographic survey using a Van Veen grab (Figure 1B,C; Table S1 in the online supplementary materials). The upper centimeter was subsampled (~1 cm) and shows good preservation of the sediment/water interface with minimal bioturbation. Note that these samples may represent different time intervals, depending on their location in the gulf. For example, the sedimentation rates (AMS-¹⁴C ages) measured in two sediment cores collected in the gulf have been estimated between 14 cm kyr⁻¹ and 24 cm kyr⁻¹ (Desiage et al., 2016). As a result, the first centimeter could represent between 40 years and 70 years of sedimentation. Thus, we consider that all sediments deposited during the last ~70 years are representative of “modern” conditions.

Palynological Sample Preparation

The protocol described by Rochon et al. (1999) was used for palynological preparations. A volume of 5 cm³ was collected by displacement of an equal volume of distilled water in a graduated cylinder and weighed using a Mettler PE 160 precision balance. A small amount of sediment was air-dried and weighed to measure the sediment water content. Two tablets of *Lycopodium clavatum* (concentration per tablet 12,100 ± 1,892, Batch 414831, University of Lund) were added to the sediment prior to chemical treatment to determine palynomorph concentrations. The sediment was then sieved at 100 μm and 10 μm using Nitex

membranes to remove coarse sands, fine silts, and clays. The fraction between 100 μm and 10 μm was treated alternately with warm hydrochloric acid (HCl, 10%) and warm hydrofluoric acid (HF, 49%) to remove the carbonates and the siliceous fraction, respectively. These warm 10-minute HCl and HF (~45°C) treatments were repeated alternately three times, with the exception of one of the HF treatments, which was done overnight (~8 hours). A fourth and final treatment with warm HCl was performed at the end to dissolve the fluorosilicate gels produced during the acid treatments. The final residue was sieved at 10 μm to remove fine particles, and then transferred to a 15 ml conical bottom tube. For mounting the slides, the 15 ml tubes were centrifuged at ~2,500 rpm for 10 minutes. The supernatant was removed and the residue homogenized for a few seconds on a vortimixer. A drop was then extracted and mounted between a slide and a coverslip in glycerine gelatin for observation under a microscope. Finally, a drop of phenol was added to the palynological residue, which was then stored at 4°C.

Palynomorph Counts

The counts were performed using a transmitted light microscope (Nikon Eclipse 80i) at ×400 magnification. Palynomorph concentrations are expressed per dry weight (cysts g⁻¹) to eliminate the influence of sediment water content (Dale, 2001), and the relative abundance of taxa is estimated in each sample (% dinocyst sp.). A minimum of 300 dinocysts or marker grains (*Lycopodium clavatum*) was counted to obtain the best statistical representation of the different species present in the samples (Table S1). All dinocysts were identified at the species level except for *Dubridinium* sp. and *Echinidinium* sp. because of morphological similarities that often prevent identification of these brown spiny cysts to the species level. The brown spiny cysts found were named *Echinidium* sp.C and sp.D in the expectation of further study (Figures S2 and S3). *Brigantedinium* spp.

includes all cysts of *Brigantedinium* where the cyst orientation did not permit clear observation of the archeopyle. Cysts of *Polykrikos kofoidii/schwartzii* were identified following Rochon et al. (1999). We also distinguished *Operculodinium centrocarpum sensu* Wall and Dale (1966) and *Operculodinium centrocapum* short processes. Pollen grains and spores, pre-Quaternary (reworked) palynomorphs (dinocyst, pollen grains, and spores), *Halodinium*, and organic linings of foraminifers were counted.

Statistical Analyses

Sampling sites were arranged in a hierarchical cluster using the relative abundance of each taxon (% dinocyst sp.) to determine dinocyst assemblage zones. The analyses were run on Past for Windows software (version 3.18) using the UPGMA (Unweighted Pair-Group average) function. Clusters are joined based on the Euclidean distance between all sites. Redundancy analyses (RDA) were performed to quantify trends in the abundance of dinocysts in relation to oceanic parameters and grain size data. These multivariate analyses are based on transformed data on the relative abundance and concentrations of dinocysts. Hellinger transformations ($\sqrt{\%}$) are done to decrease the variations between rare and dominant taxa (Legendre and Gallagher, 2001). The analyses were run using R software for Windows (R version 3.4.2). Environmental variables significantly influence species distribution when $p < 0.05$.

Environmental and Grain Size Data

Temperature and salinity data, as well as phosphate, silicate, and nitrate (μmol L⁻¹) concentrations, covering the period 1955–2012, were collected from the 2013 World Ocean Atlas database (World Ocean Atlas 2013: WOA13) from the National Oceanographic Data Center (<https://www.nodc.noaa.gov/OC5/woa13/woa13data.html>, Table S1). The data were collected on a grid of 0.25° (temperature and salinity) or 1° (phosphate,

silicate, and nitrate). When there were no data at or near our sites, the inverse distance weighted (IDW) interpolation method with ArcGIS software was used to calculate weighted averages from the values of a number of neighboring points.

Data on chlorophyll-*a* concentrations (mg m^{-3}) were extracted from Rivas et al. (2006). They were estimated from SeaWiFS processed data and correspond to the period January 1998 to December 2003 (six years). These data come from the Distributed Active Archive Center (DAAC) of the Goddard Space Flight Center (Table S1). For more information on data processing, see Rivas et al. (2006).

Particle size analysis was carried out using a Beckman Coulter Particle Size Analyzer LS 13 320 at ISMER. Prior to analysis, the samples were treated with 10 ml of hydrogen peroxide (H_2O_2 ; 30%) and 10 ml of hydrochloric acid (HCl; 0.5 M) to remove organic matter and carbonates. Samples were deflocculated by successive washing with distilled water, and put in an overhead shaker for 12 hours (overnight) before measurement (Desiagi et al., 2018, in this issue).

RESULTS

Palynomorph preservation was good to excellent in most samples. Although some taxa (e.g., *Brigantedinium* sp., *Echinidinium* sp.) can be very sensitive

to oxidation (Zonneveld et al., 2001b), none of the oxidation-sensitive taxa present in the samples showed signs of degradation. In addition, the low abundance of reworked palynomorphs suggests that there were few allochthonous sediment inputs. This indicates that the cysts found in our samples represent local productivity and that long-distance transport of dinocysts did not significantly affect the composition of the assemblages described below.

Dinocyst concentrations in the study area varied between 64 cysts g^{-1} and $45,848 \text{ cysts g}^{-1}$, with an average of $12,858 \text{ cysts g}^{-1}$. These concentrations increased along a north-south gradient in the gulf, and minimum concentrations were recorded at offshore sites (BV52, 54, 55; Figures 2 and 3). The ratio of autotrophic to heterotrophic dinocysts varied between 20.97 and 0.37, with an average of 3.84, revealing the overall dominance of autotrophic dinocysts in the SJG. The maximum abundances of heterotrophic dinocysts were recorded in the northern part of the SJG and at offshore sites (Figure 4).

Concentrations of reworked palynomorphs are low in the SJG, with an average of 135 cells g^{-1} . Maximum concentrations ($\sim 1,053 \text{ cells g}^{-1}$) are found at the gulf's outer limit (sites BV50 and BV51), and then gradually decrease

offshore. Concentrations of organic linings of foraminifera are high in the inner part of the gulf, reaching $2,018 \text{ g}^{-1}$, with an overall average of $748 \text{ linings g}^{-1}$. *Halodinium* sp., described originally as an acritarch (Bujak, 1984) and now confirmed as the resting cyst of an estuarine ciliate (Gurdebeke et al., 2018), are more abundant in the central and southern SJG, with a maximum value of 102 cells g^{-1} at site BV50, and low concentrations in the northern part of the gulf and offshore. This taxon suggests freshwater inputs to in our study area. The high concentrations of *Halodinium* sp. in central and southern SJG are correlated with the influence of freshwater discharge by the rivers located south of the gulf and carried into the SJG by coastal currents (Figure 1A). The abundance of this palynomorph in the gulf would therefore be a good proxy for documenting the fluctuations of freshwater inputs in paleoceanographic reconstructions.

In total, 30 dinocyst taxa were identified and 11 taxa dominate the assemblages by more than 90%: *Spiniferites ramosus*, *Spiniferites mirabilis*, *Operculodinium centrocarpum*, *Alexandrium* cf. *catenella*, *Impagidinium paradoxum*, *Echinidinium* sp.C, *Brigantedinium simplex*, *Brigantedinium auranteum*, *Brigantedinium* spp., *Dubridinium* sp., and cysts of *Polykrikos kofoidii* (Tables S2 and S3, Figures S1–S3).

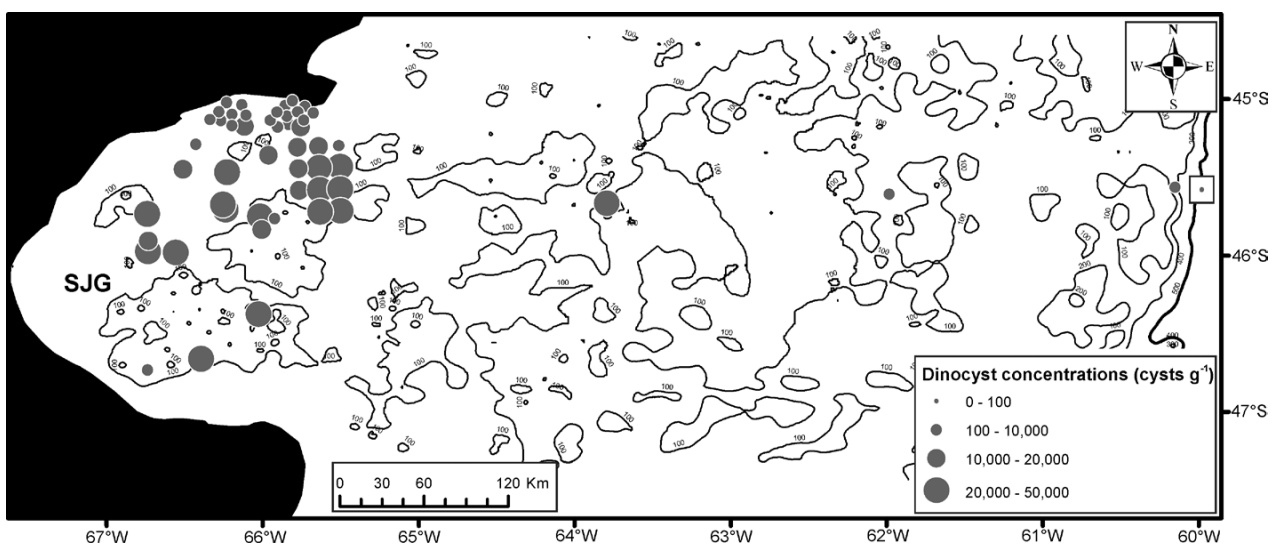


FIGURE 2. Distribution map of dinocyst concentrations (cysts g^{-1}).

Cluster statistical analysis performed with Past indicates the presence of two dinocyst assemblage zones (Figure 3). Zone I includes stations situated in the SJG that are then divided into two sub-assemblages, Ia and Ib. Dinocyst sub-assemblage zone Ia is located in the

northern part of the SJG near the coast (31–90 m water depth). The concentrations in this assemblage vary between 480 cysts g⁻¹ and 13,160 cysts g⁻¹, with an average of 3,924 cysts g⁻¹, and *Spiniferites ramosus* (16%–60%) and *O. centrocarpum* (3%–14%) are the dominant species.

The heterotrophic dinocysts, such as those of *Polykrikos kofoidii* (11%–39%), *Echinidinium* sp.C (0.6%–12%), and *Brigantedinium auranteum* (1.8%–6.9%), are also relatively abundant in this assemblage (Figures 3 and 4).

It is interesting to note that the

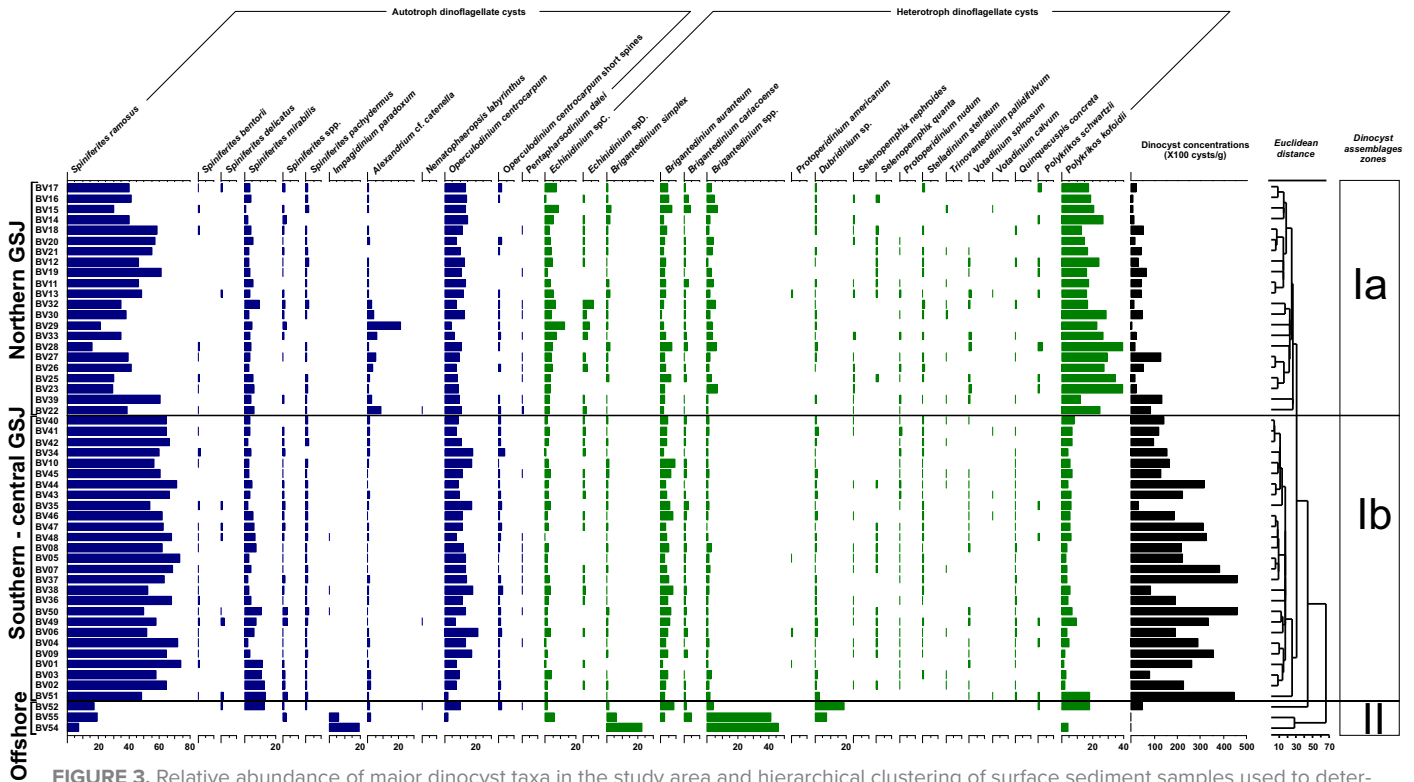


FIGURE 3. Relative abundance of major dinocyst taxa in the study area and hierarchical clustering of surface sediment samples used to determine dinocyst assemblages.

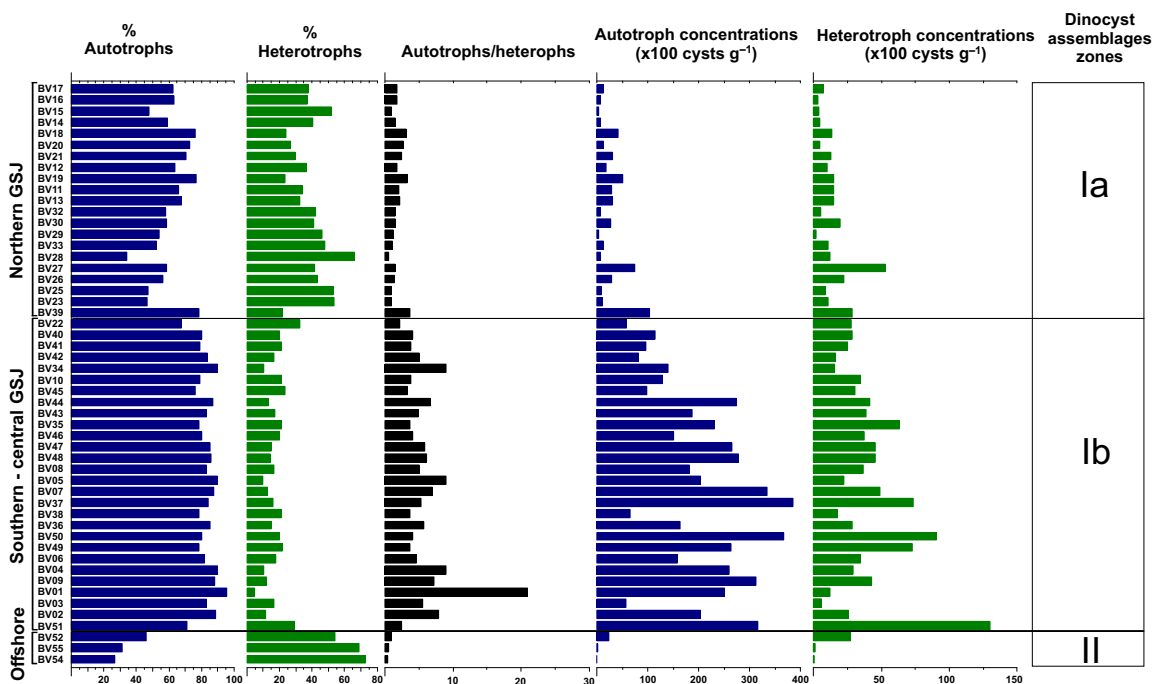


FIGURE 4. Relative abundances and ratios for autotrophic and heterotrophic dinocysts.

relative abundance of cysts of the toxin-producing species *Alexandrium* cf. *catenella* (Fabro et al., 2018, in this issue) can reach as high as 21% in this assemblage zone (Ia). The toxic dinoflagellate responsible for paralytic shellfish poisoning in the Argentinean Sea was originally described as *Alexandrium excavata*, then changed to *Alexandrium tamarense*, and more recently to *Alexandrium catenella*, based on phylogenetic reconstructions of rDNA (Fabro et al., 2017, 2018, in this issue; Krock et al., 2018, in this issue). However, *Alexandrium* cysts may have been confused with the organic linings of *Scrippsiella trifida* in previous palynological investigations (Head et al., 2006). Indeed, all *Alexandrium* cysts have similar morphology and poor fossilization potential, and are virtually absent from geological records. In addition, the acids used in standard palynological treatments can damage their cell walls (Head et al., 2006). In the present study, we observed several sediment samples prior to chemical treatments and found numerous cysts of *Alexandrium* cf. *catenella*, the majority with cellular content

(Figure S1, panels 7–10). In the processed samples, we also observed cysts of *A.* cf. *catenella*, sometimes with cellular content, but their abundance may have been underestimated because of the problems mentioned earlier.

Subassemblage zone Ib includes stations located in the central and southern part of the SJG (80–100 m water depth). Dinocyst concentrations are maximum and range between 8,268 cysts g⁻¹ and 45,848 cysts g⁻¹. The dominant taxa are *S. ramosus* (49%–74%), *O. centrocarpum* (6%–21%), and *S. mirabilis* (2%–12%). Autotrophic dinocysts dominate this subassemblage, and heterotrophic dinocysts are relatively lower in abundance. The most abundant heterotrophic dinocysts are those of *P. kofoidii* (1%–9%) and the *Echinidium* sp.C (0.5%–3.9%; Figures 3 and 4).

Assemblage zone II regroups the four samples located offshore (108–647 m water depth). Concentrations are relatively low, ranging from 64 cysts g⁻¹ to 5,026 cysts g⁻¹, in contrast to assemblage zone I. Heterotrophic dinocysts dominate this assemblage and are represented

by *Brigantedinium* spp. (4%–46%), cysts of *P. kofoidii* (0%–17%), and *Dubridinium* sp. (0%–18%). The oceanic species *Impagidinium paradoxum* also appears here and can reach a maximum of 19%. In addition, the relative abundance of autotrophic dinocysts is low compared to assemblage I (Figures 3 and 4): *S. ramosus* registers at 7%–19%, *O. centrocarpum* at 0%–10%, and *S. mirabilis* at 0%–12%.

RDA analyses were performed with all variables and with single explanatory variables for relative abundance and concentration data. The RDA results reveal the same sample groupings as those from the cluster analyses. Many environmental variables are statically significant ($p < 0.05$) when they are used as sole explanatory variables or together (Table S4, Figure 5).

For relative abundance (%) analyses, chlorophyll-*a* concentrations in March (ch.a.m, austral autumn), August (Ch.a.a, austral winter), and November (Ch.a.n, austral spring); temperature and salinity in winter and summer (T.win, T.sum, S.win, S.sum); and annual concentrations of nitrate (N) and phosphate (P) all

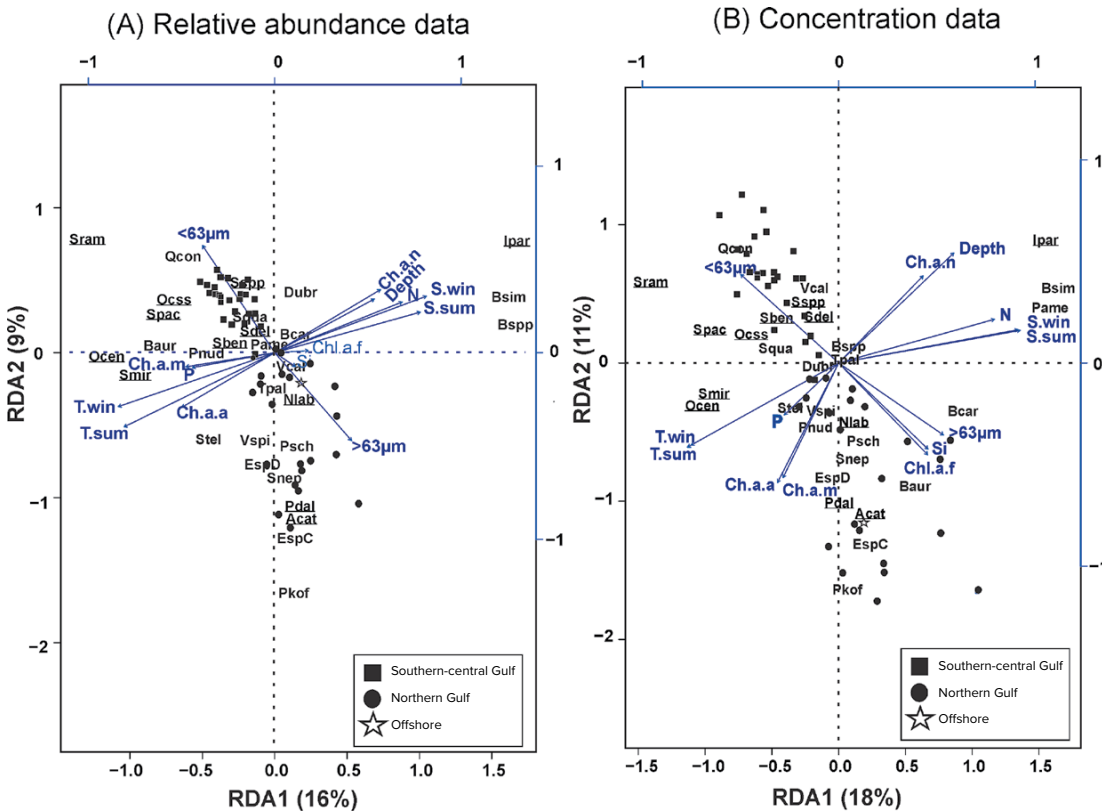


FIGURE 5. Correlation biplot based on redundancy analysis (RDA) for dinocyst assemblages, sea surface parameters, grain size data (fraction > 63 µm and < 63 µm) and depth. Winter and summer temperature (T.win, T.sum), summer salinity (S.sum), nitrate (N), phosphate (P) concentrations, and chlorophyll-*a* concentrations (February = Ch.a.f, May = Ch.a.m, August = Ch.a.a, November = Ch.a.n). RDA run with (A) relative abundance of cysts, and (B) concentration data. A variable is statically significant if $p < 0.05$. Variable axes are in blue. Autotrophic dinocysts are underlined.

contribute significantly to defining assemblage compositions ($p < 0.05$). Northern SJG sites (subassemblage Ia) correlate with heterotrophic dinocysts (cysts of *P. kofoidii* and *P. schwartzii*, *Echinidinium* sp.C, *Echinidinium* sp.D, *Selenopemphix nephroides*, *Trinovantedinium pallidifulum* and *Votadinium spinosum*). However, sites located in the central and southern SJG (subassemblage zone Ib) do not seem to be associated with any environmental variable (in the two RDA analyses), but correlate with autotrophic dinocysts and with fine particle size ($> 63 \mu\text{m}$) in surface sediments (Figure 5A).

In concentration analysis, we find the same patterns: the northern sites (subassemblage zone Ia) are associated with Ch.a.f (1.7 mg m^{-3} on average), Ch.a.m (1.6 mg m^{-3} on average), Ch.a.a (1.2 mg m^{-3} on average), Si ($34.9 \mu\text{mol L}^{-1}$), and surface temperature ($\sim 8.5^\circ\text{C}$ during austral winter and 14.9°C during austral summer). Salinity (~ 33.4) in the SJG seems to have a weak influence on the distribution of dinocysts. The main finding in this analysis is a negative correlation between Si and southern-central sites (Figure 5B). It is also noted in the two RDA triplots that round brown cysts (*Brigantedinium simplex* and *Brigantedinium* spp.) and *I. paradoxum* correlate with water depth (Figure 5).

DISCUSSION

Relatively high dinocyst concentrations (maximum $45,848 \text{ cysts g}^{-1}$ and average $12,858 \text{ cysts g}^{-1}$) can be related to fine particle size in surface sediments in the southern-central gulf (Figures 4 and 5). Indeed, dinocysts are the same size as silt particles and exhibit similar hydrodynamic behavior, so they tend to be concentrated with fine sediments (e.g., Dale, 1976). In general, two spatial domains emerge from the distribution of dinocysts in the SJG (northern/south-central gulf and offshore domains). Autotrophic dinocysts dominate the assemblages because of the high primary productivity that characterizes the Southwest Atlantic Ocean (Figure 1A). The increase

in dinoflagellate cyst concentrations along a north-south gradient in the SJG is most likely due to the input of nutrient-rich subantarctic waters via the Patagonia Current (Figure 1A), which promotes the development of dinoflagellate species in southern-central SJG (subassemblage zone Ib). The production of dinocysts appears to be controlled in the north by productivity during austral summer (Ch.a.f), autumn (Ch.a.m), and winter (Ch.a.a), and by surface temperatures (Figure 5).

The high relative abundance of heterotrophic dinocysts in subassemblage Ia in the northern SJG may be related to the presence of diatoms found in the northern part of the gulf (Krock et al., 2015; Latorre, 2018). Indeed, diatoms are the main prey for some heterotrophic dinoflagellates (Jacobson and Anderson, 1986; Hansen, 1992; Jeong et al., 2010). This concept is supported by the relatively high Si concentrations ($40.5\text{--}41.5 \mu\text{mol L}^{-1}$) found at stations BV11, 14, 13, 15, 16, 19, and 20, which could promote the development of diatoms (e.g., Dugdale and Wilkerson, 2001). In addition, Smayda, (1997) showed that the presence of diatoms is more important than that of dinoflagellates in turbulent zones (such as in the northern gulf) because their cell structures are adapted to this type of environment, and also because of their competitiveness in the battle for nutrients. Regarding the food web structure in the northern gulf, the high abundance of cysts of *Polykrikos kofoidii* (11%–39%) is interesting because this species is known to feed on a large variety of prey, including other SJG dinoflagellates such as *Gonyaulax spinifera* and *Alexandrium* species (Matsuoka et al., 2000). Diatoms and dinoflagellates could therefore be a food source for heterotrophic dinoflagellates.

The high abundance of dinocysts in the central and southern SJG may be due to the stratified nature of the water column in the central part of the basin (e.g., Krock et al., 2015) and the presence of a tidal front in the area (Figure 1A; Rivas et al.,

2006, Carbajal et al., 2018, in this issue). Stratified waters favor the development of dinoflagellates, whose two flagella allow them to migrate vertically and obtain the nutrients necessary for their survival at depth (Smayda et al., 1997). The high abundance of autotrophic dinocysts in this subassemblage could be explained by the decreasing trend of Si from north to south, which would favor the development of autotrophic dinoflagellates over diatoms (e.g., Smayda, 1990).

The low abundance of dinocysts at offshore sites (assemblage zone II) is similar to other observations of dinocyst distributions in the global ocean (Zonneveld et al., 2013). The ubiquitous genera *Spiniferites* and *Operculodinium*, which are the major contributors to northern and southern-central assemblages, are found preferentially in nutrient-rich coastal waters. In addition, high offshore concentrations of heterotrophic dinocysts are associated with the upwelling around the 200 m isobath (Matano et al., 2010) that promotes high biological productivity and permits the development of primary producers such as diatoms that serve as prey for heterotrophic dinoflagellates. This is corroborated by the high abundance at the offshore sites (BV54, BV55) of round brown cysts (*Brigantedinium* spp., *Brigantedinium simplex*), whose presence is an indicator of high productivity areas such as upwelling zones (e.g., Zonneveld et al., 2001a, Pospelova et al., 2008). The presence of *Impagidinium paradoxum* is strongly correlated to water depth (Figure 5). This taxon is considered to be an oceanic species (Zonneveld et al., 2013).

CONCLUSIONS

This study, based on the analysis of 52 surface sediment samples, provides the first detailed description of the distribution of modern dinoflagellate cyst assemblages in the SJG. Two assemblage zones were identified from the relative abundances of dinocysts and from hierarchical clustering and RDA analyses. The distribution of dinocysts appears to be primarily

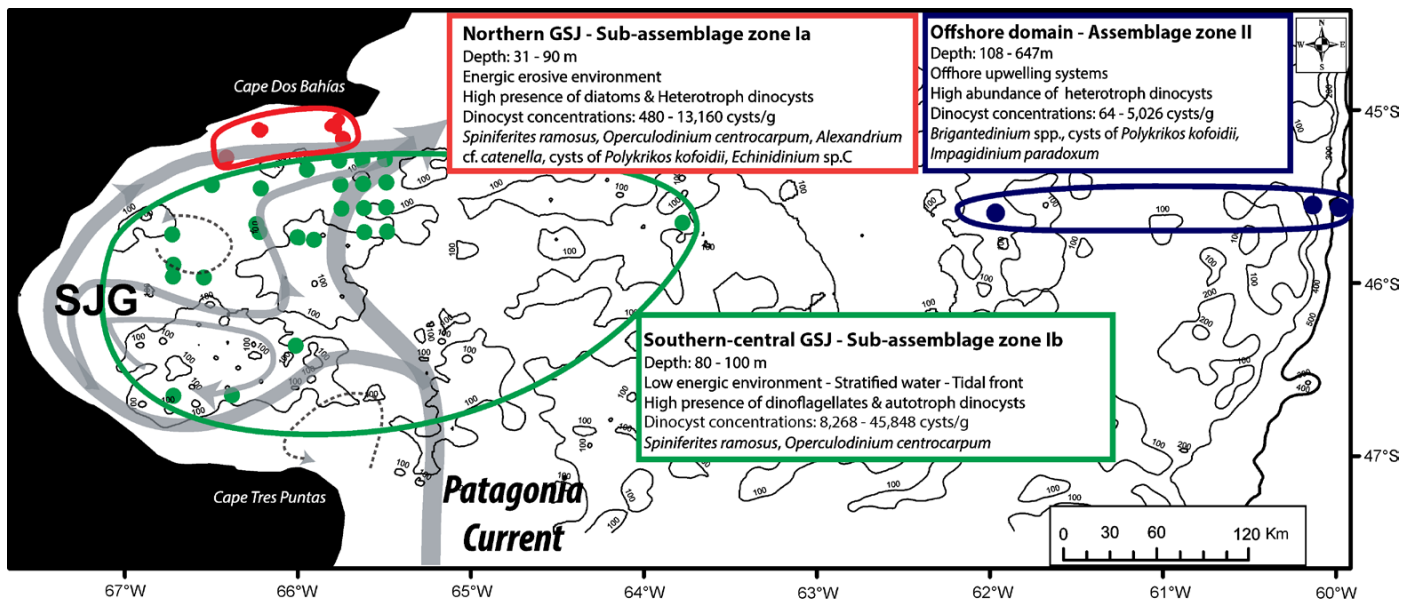


FIGURE 6. Spatial distribution of dinocyst assemblages in the SJG and code name used in Figure 5 and Table S3.

controlled by local primary productivity and offshore upwelling. Dinocyst concentrations are high in the southern-central gulf, where we note the fine particle size of surface sediments. The concentrations of dinocysts increase along a north-south gradient in the SJG, with minimum concentrations at offshore sites (outside the gulf). The high concentrations of dinocysts in the southern-central gulf are associated with the input of nutrient-rich subantarctic water, water column stratification, and tidal fronts in the southern part of the gulf. The presence of heterotrophic dinocysts in the northern SJG and offshore is related to prey availability and upwelling (Figure 6). Dinocysts are an important part of the organic carbon preserved in SJG sediments, and thus represent an important indicator of primary paleo-productivity that can be used in paleoceanographic reconstructions. 📄

SUPPLEMENTARY MATERIALS

Supplementary materials are available online at <https://doi.org/10.5670/oceanog.2018.416>.

REFERENCES

Aravena, J.-C., and B.H. Luckman. 2009. Spatio-temporal rainfall patterns in Southern South America. *International Journal of Climatology* 29(14):2,106–2,120, <https://doi.org/10.1002/joc.1761>.

Bianchi, A.A. 2005. Vertical stratification and air-sea CO₂ fluxes in the Patagonian shelf. *Journal of Geophysical Research* 110(C7), <https://doi.org/10.1029/2004JC002488>.

Bogus, K., K.N. Mertens, J. Lauwaert, I.C. Harding, H. Vrielinck, K.A. Zonneveld, and G.J. Versteegh. 2014. Differences in the chemical composition of organic-walled dinoflagellate resting cysts from phototrophic and heterotrophic dinoflagellates. *Journal of Phycology* 50(2):254–266, <https://doi.org/10.1111/jpy.12170>.

Brandhorst, W., and J.P. Castello. 1971. *Evaluación de los Recursos de Anchoíta (Engraulis anchoíta) frente a la Argentina y Uruguay*. Serie de Informaciones Técnicas 29, Proy. Des. Pesquero (FAO), 63 pp.

Bujak, J.P. 1984. Cenozoic dinoflagellate cysts and acritarchs from the Bering Sea and northern North Pacific, DSDP Leg 19. *Micropaleontology* 30(2):180–212.

Candel, M.S., T. Radi, A. de Vernal, and G. Bujalesky. 2012. Distribution of dinoflagellate cysts and other aquatic palynomorphs in surface sediments from the Beagle Channel, Southern Argentina. *Marine Micropaleontology* 96–97:1–12, <https://doi.org/10.1016/j.marmicro.2012.06.009>.

Carbajal, J.C., A.L. Rivas, and C. Chavanne. 2018. High-frequency frontal displacements south of San Jorge Gulf during a tidal cycle near spring and neap phases: Biological implications between tidal states. *Oceanography* 31(4):60–69, <https://doi.org/10.5670/oceanog.2018.411>.

Dale, B. 1976. Cyst formation, sedimentation, and preservation: Factors affecting dinoflagellate assemblages in recent sediments from Trondheimsfjord, Norway. *Review of Palaeobotany and Palynology* 22(1):39–60, [https://doi.org/10.1016/0034-6667\(76\)90010-5](https://doi.org/10.1016/0034-6667(76)90010-5).

Dale, B. 2001. Marine dinoflagellate cysts as indicators of eutrophication and industrial pollution: A discussion. *Science of the Total Environment* 264(3):235–240, [https://doi.org/10.1016/S0048-9697\(00\)00719-1](https://doi.org/10.1016/S0048-9697(00)00719-1).

Desiège, P.-A., J.-C. Montero-Serrano, G. St-Onge, A.C. Crespi-Abril, E. Giarratano, M.N. Gil, and M.J. Haller. 2018. Quantifying sources and transport pathways of surface sediments in the Gulf of San Jorge, central Patagonia (Argentina). *Oceanography* 31(4):92–103, <https://doi.org/10.5670/oceanog.2018.401>.

Desiège, P.-A., G. St-Onge, J.-C. Montero-Serrano, M.J. Duchesne, and M. Haller. 2016. Late Pleistocene and Holocene sea-level variations and post-glacial sedimentation in the Gulf of San Jorge (Argentina, Central Patagonia). Poster session presented at the Fall Meeting of the American Geophysical Union.

de Vernal, A., A. Rochon, B. Fréchette, M. Henry, T. Radi, and S. Solignac. 2013. Reconstructing past sea ice cover of the Northern Hemisphere from dinocyst assemblages: Status of the approach. *Quaternary Science Reviews* 79:122–134, <https://doi.org/10.1016/j.quascirev.2013.06.022>.

Dugdale, R.C., and F.P. Wilkerson. 2001. Sources and fates of silicon in the ocean: The role of diatoms in the climate and glacial cycles. *Scientia Marina* 65(S2):141–152, <https://doi.org/10.3989/scimar.200165s2141>.

Durantou, L., A. Rochon, D. Ledu, G. Massé, S. Schmidt, and M. Babin. 2012. Quantitative reconstruction of sea-surface conditions over the last 150 yr in the Beaufort Sea based on dinoflagellate cyst assemblages: The role of large-scale atmospheric circulation patterns. *Biogeosciences* 9(12):5,391–5,406, <https://doi.org/10.5194/bg-9-5391-2012>.

Esper, O., and K.A.F. Zonneveld. 2002. Distribution of organic-walled dinoflagellate cysts in surface sediments of the Southern Ocean (eastern Atlantic sector) between the Subtropical Front and the Weddell Gyre. *Marine Micropaleontology* 46(1):177–208, [https://doi.org/10.1016/S0377-8398\(02\)00041-5](https://doi.org/10.1016/S0377-8398(02)00041-5).

Evitt, W.R. 1985. *Sporopollenin Dinoflagellate Cysts: Their Morphology and Interpretation*. American Association of Stratigraphic Palynologists Foundation, Dallas, 333 pp.

Fabro, E., G.O. Almandoz, M. Ferrario, U. John, U. Tillmann, K. Toebe, B. Krock, and A. Cembella. 2017. Morphological, molecular, and toxin analysis of field populations of *Alexandrium* genus from the Argentine Sea. *Journal of Phycology* 53(6):1,206–1,222, <https://doi.org/10.1111/jpy.12574>.

Fabro, E., B. Krock, A.I. Torres, F.E. Papparazzo, I.R. Schloss, G.A. Ferreyra, and G.O. Almandoz. 2018. Toxicogenic dinoflagellates and associated toxins in San Jorge Gulf, Argentina. *Oceanography* 31(4):145–153, <https://doi.org/10.5670/oceanog.2018.417>.

Fernández, M., A. Roux, E. Fernández, J. Caló, A. Marcos, and H. Aldacur. 2003. Grain-size analysis of surficial sediments from Golfo San Jorge, Argentina. *Journal of the Marine Biological Association of the United Kingdom* 83(6):1,193–1,197, <https://doi.org/10.1017/S0025315403008488>.

Glembocik, N.G., G.N. Williams, M.E. Góngora, D.A. Gagliardini, and J.M. (Lobo) Orensanz. 2015. Synoptic oceanography of San Jorge Gulf (Argentina): A template for Patagonian red shrimp

- (*Pleoticus muelleri*) spatial dynamics. *Journal of Sea Research* 95:22–35, <https://doi.org/10.1016/j.seares.2014.10.011>.
- Gregg, W.W. 2005. Recent trends in global ocean chlorophyll. *Geophysical Research Letters* 32(3), <https://doi.org/10.1029/2004GL021808>.
- Gruberbeke, P.R., K.N. Mertens, Y. Takano, A. Yamaguchi, K. Bogus, M. Dunthorn, K. Matsuoka, H. Vrielinck, and S. Louwye. 2018. The affiliation of *Hexasterias problematica* and *Halodinium verucatum* sp. nov. to ciliate cysts based on molecular phylogeny and cyst wall composition. *European Journal of Protistology* 66:115–135, <https://doi.org/10.1016/j.ejop.2018.09.002>.
- Hansen, P.J. 1992. Prey size selection, feeding rates and growth dynamics of heterotrophic dinoflagellates with special emphasis on *Gyrodinium spirale*. *Marine Biology* 114(2):327–334, <https://doi.org/10.1007/BF00349535>.
- Head, M.J. 1996. Modern dinoflagellate cysts and their biological affinities. Pp. 1,197–1,248 in *Palynology Principles and Applications*, vol. 3. J. Jansoni and D.C. McGregor, eds, American Association of Stratigraphic Palynologists Foundation, Dallas, TX.
- Head, M.J., J. Lewis, and A. de Vernal. 2006. The cyst of the calcareous dinoflagellate *Scripsiella trifida*: Resolving the fossil record of its organic wall with that of *Alexandrium tamarense*. *Journal of Paleontology* 80(1):1–18, [https://doi.org/10.1666/0022-3360\(2006\)080\[0001:TCOTCD\]2.0.CO;2](https://doi.org/10.1666/0022-3360(2006)080[0001:TCOTCD]2.0.CO;2).
- Jacobson, D.M., and D.M. Anderson. 1986. Thecate heterotrophic dinoflagellates: Feeding behavior and mechanisms. *Journal of Phytoplankton Research* 22(3):249–258, <https://doi.org/10.1111/j.1529-8817.1986.tb00021.x>.
- Jeong, H.-J., Y.D. Yoo, J.S. Kim, K.A. Seong, N.S. Kang, and T.H. Kim. 2010. Growth, feeding and ecological roles of the mixotrophic and heterotrophic dinoflagellates in marine planktonic food webs. *Ocean Science Journal* 45(2):65–91, <https://doi.org/10.1007/s12601-010-0007-2>.
- Krock, B., C.M. Borel, F. Barrera, U. Tillmann, E. Fabro, G.O. Almandoz, M. Ferrario, J.E. Garzón Cardona, B.P. Koch, C. Alonso, and R. Lara. 2015. Analysis of the hydrographic conditions and cyst beds in the San Jorge Gulf, Argentina, that favor dinoflagellate population development including toxicogenic species and their toxins. *Journal of Marine Systems* 148:86–100, <https://doi.org/10.1016/j.jmarsys.2015.01.006>.
- Krock, B., M.E. Ferrario, R. Akselman, and N.G. Montoya. 2018. Occurrence of marine biotoxins and shellfish poisoning events and their causative organisms in Argentine marine waters. *Oceanography* 31(4):132–144, <https://doi.org/10.5670/oceanog.2018.403>.
- Latorre, M.P. 2018. *Contrôle de la Structure et de la Distribution de la Communauté Microbienne dans le Golfe de San Jorge, Argentine*. Maitrise, Université du Québec à Rimouski, 104 pp.
- Legendre, P., and E.D. Gallagher. 2001. Ecologically meaningful transformations for ordination of species data. *Oecologia* 129(2):271–280, <https://doi.org/10.1007/s004420100716>.
- Lutz, V.A., and J. Carreto. 1991. A new spectrofluorometric method for the determination of chlorophylls and degradation products and its application in two frontal areas of the Argentine Sea. *Continental Shelf Research* 11:433–451, [https://doi.org/10.1016/0278-4343\(91\)90052-8](https://doi.org/10.1016/0278-4343(91)90052-8).
- Matano, R.P., and E.D. Palma. 2018. Seasonal variability of the oceanic circulation in the Gulf of San Jorge, Argentina. *Oceanography* 31(4):16–24, <https://doi.org/10.5670/oceanog.2018.402>.
- Matano, R.P., E.D. Palma, and A.R. Piola. 2010. The influence of the Brazil and Malvinas Currents on the Southwestern Atlantic Shelf circulation. *Ocean Science* 6(4):983–995, <https://doi.org/10.5194/os-6-983-2010>.
- Matsuoka, K., H.J. Cho, and D.M. Jacobson. 2000. Observations of the feeding behavior and growth rates of the heterotrophic dinoflagellate *Polykrikos kofoidii* (Polykrikaceae, Dinophyceae). *Phycologia* 39(1):82–86, <https://doi.org/10.2216/i0031-8884-39-1-82.1>.
- Mayr, C., M. Wille, T. Haberzettl, M. Fey, S. Janssen, A. Lucke, C. Ohlendorf, G. Oliva, F. Schabitz, and G. Schleser. 2007. Holocene variability of the Southern Hemisphere westerlies in Argentinean Patagonia (52°S). *Quaternary Science Reviews* 26(5–6):579–584, <https://doi.org/10.1016/j.quascirev.2006.11.013>.
- Orozco, F.E., and J.I. Carreto. 1989. Distribution of *Alexandrium excavatum* resting cysts in a Patagonian shelf area (Argentina). Pp. 309–312 in *Red Tides: Biology, Environmental Science and Toxicology*, T. Okaichi, D.M. Anderson, and T. Nemoro, eds, Elsevier Science Publishing.
- Palma, E.D., R.P. Matano, and A.R. Piola. 2008. A numerical study of the Southwestern Atlantic Shelf circulation: Stratified ocean response to local and offshore forcing. *Journal of Geophysical Research* 113(C11), <https://doi.org/10.1029/2007JC004720>.
- Piola, A.R., N.M. Avellaneda, R.A. Guerrero, F.P. Jardón, E.D. Palma, and S.I. Romero. 2009. Malvinas-slope water intrusions on the northern Patagonia continental shelf. *Ocean Science Discussions* 6(4):345–359, <https://doi.org/10.5194/os-6-345-2010>.
- Pospelova, V., A. de Vernal, and T.F. Pedersen. 2008. Distribution of dinoflagellate cysts in surface sediments from the northeastern Pacific Ocean (43–25°N) in relation to sea-surface temperature, salinity, productivity and coastal upwelling. *Marine Micropaleontology* 68(1–2):21–48, <https://doi.org/10.1016/j.marmicro.2008.01.008>.
- Rivas, A.L., A.I. Dogliotti, and D.A. Gagliardini. 2006. Seasonal variability in satellite-measured surface chlorophyll in the Patagonian Shelf. *Continental Shelf Research* 26(6):703–720, <https://doi.org/10.1016/j.csr.2006.01.013>.
- Rochon, A., A.D. Vernal, J.L. Turon, J. Matthiessen, and M.J. Head. 1999. Distribution of recent dinoflagellate cysts in surface sediments from the North Atlantic Ocean and adjacent seas in relation to sea-surface parameters. *American Association of Stratigraphic Palynologists Contribution Series* 35:1–146.
- Sabatini, M., and P. Martos. 2002. Mesozooplankton features in a frontal area off northern Patagonia (Argentina) during spring 1995 and 1998. *Scientia Marina* 66:215–232, <https://doi.org/10.3989/scimar.2002.66n3215>.
- Segura, V., V. Lutz, A. Dogliotti, R. Silva, R. Negri, R. Akselman, and H. Benavides. 2013. Phytoplankton types and primary production in the Argentine Sea. *Marine Ecology Progress Series* 491:15–31, <https://doi.org/10.3354/meps10461>.
- Smayda, T.J. 1990. Novel and nuisance phytoplankton blooms in the sea: Evidence for a global epidemic. Pp. 29–40 in *Toxic Marine Phytoplankton*. E. Granéli, B. Sundström, L. Edler, and D.M. Anderson, eds, Elsevier.
- Smayda, T.J. 1997. Harmful algal blooms: Their ecophysiology and general relevance to phytoplankton blooms in the sea. *Limnology and Oceanography* 42(5, part2):1137–1153, https://doi.org/10.4319/lo.1997.42.5_part_2.1137.
- Stoecker, D.K. 1999. Mixotrophy among dinoflagellates. *Journal of Eukaryotic Microbiology* 46(4):397–401, <https://doi.org/10.1111/j.1550-7408.1999.tb04619.x>.
- Taylor, F.J.R., M. Hoppenrath, and J.F. Saldarriaga. 2008. Dinoflagellate diversity and distribution. *Biodiversity and Conservation* 17(2):407–418, <https://doi.org/10.1007/s10531-007-9258-3>.
- Tonini, M.H., E.D. Palma, and A. Rivas. 2006. Modelo de alta resolución de los golfos norpatagónicos. *Mecánica Computacional XXV*:1,441–1,460.
- Versteegh, G.J.M., P. Blokker, K.A. Bogus, I.C. Harding, J. Lewis, S. Oltmanns, A. Rochon, and K.A.F. Zonneveld. 2012. Infra red spectroscopy, flash pyrolysis, thermally assisted hydrolysis and methylation (THM) in the presence of tetramethylammonium hydroxide (TMAH) of cultured and sediment-derived *Lingulodinium polyedrum* (Dinoflagellata) cyst walls. *Organic Geochemistry* 43:92–102, <https://doi.org/10.1016/j.orggeochem.2011.10.007>.
- Wall, D., B. Dale, G.P. Lohmann, and W.K. Smith. 1977. The environmental and climatic distribution of dinoflagellate cysts in modern marine sediments from regions in the North and South Atlantic Ocean and adjacent seas. *Marine Micropaleontology* 2:121–200, [https://doi.org/10.1016/0377-8398\(77\)90008-1](https://doi.org/10.1016/0377-8398(77)90008-1).
- Zonneveld, K.A., R.P. Hoek, H. Brinkhuis, and H. Willems. 2001b. Geographical distributions of organic-walled dinoflagellate cysts in surficial sediments of the Benguela upwelling region and their relationship to upper ocean conditions. *Progress in Oceanography* 48(1):25–72, [https://doi.org/10.1016/S0079-6611\(00\)00047-1](https://doi.org/10.1016/S0079-6611(00)00047-1).
- Zonneveld, K.A.F., F. Marret, G.J.M. Versteegh, K. Bogus, S. Bonnet, I. Bouimetarhan, E. Crouch, A. de Vernal, R. Elshaniwany, L. Edwards, and others. 2013. Atlas of modern dinoflagellate cyst distribution based on 2405 data points. *Review of Palaeobotany and Palynology* 191:1–197, <https://doi.org/10.1016/j.revpalbo.2012.08.003>.
- Zonneveld, K.A.F., G.J.M. Versteegh, and G.J. De Lange. 2001a. Palaeoproductivity and post-depositional aerobic organic matter decay reflected by dinoflagellate cyst assemblages of the Eastern Mediterranean S1 sapropel. *Marine Geology* 172(3):181–195, [https://doi.org/10.1016/S0025-3227\(00\)00134-1](https://doi.org/10.1016/S0025-3227(00)00134-1).

ACKNOWLEDGMENTS

The authors are grateful to the captain, officers, crew, and scientists of the MARGES expedition on board R/V *Coriolis II*. We are grateful for the financial support of the Ministerio de Ciencia, Tecnología e Innovación Productiva (MINCYT), Provincia de Chubut and the Consejo Nacional de Investigaciones Científicas Técnicas (CONICET) for the MARES and MARGES expeditions. Special thanks to A. Rivas and Pierre-Arnaud Desiage, who provided chlorophyll-*a* and grain size data, respectively. We also thank the reviewers for their comments that helped improve this manuscript. This work was carried out with the financial support of FRQNT (Fonds de recherche du Québec – Nature et technologies) to G. St-Onge and A. Rochon and NSERC Discovery grants to A. Rochon and G. St-Onge.

AUTHORS

Simon Faye (simon.faye@uqar.ca) is a PhD candidate, Institut des sciences de la mer de Rimouski (ISMER), Québec Océan, and GEOTOP, Université du Québec à Rimouski, Québec, Canada. **André Rochon** is Professor, ISMER and GEOTOP, Université du Québec à Rimouski, Québec, Canada. **Guillaume St-Onge** is Professor and holds the Tier I Canada Research Chair in Marine Geology, ISMER, and GEOTOP, Université du Québec à Rimouski, Québec, Canada.

ARTICLE CITATION

Faye, S., A. Rochon, and G. St-Onge. 2018. Distribution of modern dinoflagellate cyst assemblages in surface sediments of San Jorge Gulf (Patagonia, Argentina). *Oceanography* 31(4):122–131, <https://doi.org/10.5670/oceanog.2018.416>.